



Multidimensional dynamic prediction model for hospitalized patients with the omicron variant in China

Yujie Chen^{a,2}, Yao Wang^{b,2}, Jieqing Chen^{c,2}, Xudong Ma^{d,2}, Longxiang Su^a, Yuna Wei^b, Linfeng Li^b, Dandan Ma^e, Feng Zhang^e, Wen Zhu^e, Xiaoyang Meng^e, Guoqiang Sun^e, Lian Ma^e, Huizhen Jiang^e, Chang Yin^{g,***}, Taisheng Li^{f,**}, Xiang Zhou^{a,c,*}, China National Critical Care Quality Control Center Group¹

^a Department of Critical Care Medicine, Peking Union Medical College Hospital, Chinese Academy of Medical Sciences and Peking Union Medical College, Beijing, 100730, China

^b Yidu Cloud Technology Inc., Beijing, China

^c Information Center Department, State Key Laboratory of Complex Severe and Rare Diseases, Peking Union Medical College Hospital, Peking Union Medical College and Chinese Academy of Medical Sciences, Beijing, 100730, China

^d Department of Medical Administration, National Health Commission of the People's Republic of China, Beijing, 100044, China

^e Information Center, State Key Laboratory of Complex Severe and Rare Diseases, Peking Union Medical College Hospital, Chinese Academy of Medical Sciences and Peking Union Medical College, Beijing, 100730, China

^f Department of Infectious Diseases, Peking Union Medical College Hospital, Chinese Academy of Medical Sciences, Beijing, China

^g National Institute of Hospital Administration, Beijing, China

ARTICLE INFO

Article history:

Received 24 June 2023

Received in revised form 9 September 2023

Accepted 18 September 2023

Available online 2 October 2023

Handling editor: Daihai He

Keywords:

COVID-19

Omicron

Prediction model

Machine learning

ABSTRACT

Purpose: To establish dynamic prediction models by machine learning using daily multidimensional data for coronavirus disease 2019 (COVID-19) patients.

Methods: Hospitalized COVID-19 patients at Peking Union Medical College Hospital from Nov 2nd, 2022, to Jan 13th, 2023, were enrolled in this study. The outcome was defined as deterioration or recovery of the patient's condition. Demographics, comorbidities, laboratory test results, vital signs, and treatments were used to train the model. To predict the following days, a separate XGBoost model was trained and validated. The Shapley additive explanations method was used to analyze feature importance.

Results: A total of 995 patients were enrolled, generating 7228 and 3170 observations for each prediction model. In the deterioration prediction model, the minimum area under the receiver operating characteristic curve (AUROC) for the following 7 days was 0.786 (95% CI 0.721–0.851), while the AUROC on the next day was 0.872 (0.831–0.913). In the recovery prediction model, the minimum AUROC for the following 3 days was 0.675 (0.583–0.767), while the AUROC on the next day was 0.823 (0.770–0.876). The top 5 features for

* Corresponding author. Department of Critical Care Medicine, Peking Union Medical College Hospital, Chinese Academy of Medical Sciences and Peking Union Medical College, Beijing, 100730, China.

** Corresponding author.

*** Corresponding author.

E-mail addresses: herminedoc@foxmail.com (Y. Chen), yao.wang@yiduccloud.cn (Y. Wang), chenjieqing@pumch.cn (J. Chen), 13910092912@163.com (X. Ma), slx77@163.com (L. Su), yuna.wei@yiduccloud.cn (Y. Wei), linfeng.li@yiduccloud.cn (L. Li), madandan@pumch.cn (D. Ma), zhangfeng@pumch.cn (F. Zhang), zhuwen@pumch.cn (W. Zhu), mengxy@pumch.cn (X. Meng), sungq@pumch.cn (G. Sun), mal@pumch.cn (L. Ma), jianghuizhen@pumch.cn (H. Jiang), yinchang99@163.com (C. Yin), litsh@263.net (T. Li), zx_pumc@163.com (X. Zhou).

Peer review under responsibility of KeAi Communications Co., Ltd.

¹ Monitored email of China National Critical Care Quality Control Center group. china_nccc@163.com.

² These authors contributed to the work equally.

<https://doi.org/10.1016/j.idm.2023.09.003>

2468-0427/© 2023 The Authors. Publishing services by Elsevier B.V. on behalf of KeAi Communications Co. Ltd. This is an open access article under the CC BY-NC-ND license (<http://creativecommons.org/licenses/by-nc-nd/4.0/>).

deterioration prediction on the 7th day were disease course, length of hospital stay, hypertension, and diastolic blood pressure. Those for recovery prediction on the 3rd day were age, D-dimer levels, disease course, creatinine levels and corticosteroid therapy.

Conclusion: The models could accurately predict the dynamics of Omicron patients' conditions using daily multidimensional variables, revealing important features including comorbidities (e.g., hyperlipidemia), age, disease course, vital signs, D-dimer levels, corticosteroid therapy and oxygen therapy.

© 2023 The Authors. Publishing services by Elsevier B.V. on behalf of KeAi Communications Co. Ltd. This is an open access article under the CC BY-NC-ND license (<http://creativecommons.org/licenses/by-nc-nd/4.0/>).

1. Background

Coronavirus disease 2019 (COVID-19) has been the most serious global public health crisis in recent years, with many cases of multiple organ dysfunction syndrome (MODS) due to severe acute respiratory syndrome coronavirus 2 (SARS-CoV-2), leading to a major challenge of severe depletion of healthcare resources and many patient deaths. Similar to all critically ill patients, the key to rescuing critically ill COVID-19 patients is to identify the signs of deterioration early.

Although numerous studies have tried to predict the risks borne by COVID-19 patients, there are still unmet challenges. Most previous studies used patient status at some fixed time point (usually at admission) (Assaf et al., 2020; Gao et al., 2020) or used only a limited dimension of longitudinal clinical status, e.g., only laboratory tests (Kogan et al., 2022), to predict the risk of deterioration or death. However, a patient outcome is determined by the interaction of viral invasion and replication process, immune response intensity, underlying physical condition, disease progression, state of organ dysfunction, and the timing, manner, and intensity of clinical treatments, which are constantly evolving. Due to limitations in their designs, neither predictive models using fixed time cross-sectional variables nor models using time series of limited factors can scientifically and completely reflect the dynamic changes of patients in the real world.

Therefore, our study collected data on the daily course, including the patient's inflammatory response, the underlying physical condition, the state of organ dysfunction, and the timing, manner, and intensity of clinical intervention after these Omicron patients started receiving care, to accurately portray the evolution of the patient's condition as these factors continued to interact and to develop dynamic prediction models (deterioration model and recovery model) to provide an earlier warning of changes in the patient condition and to identify key predictive features.

2. Method

2.1. Overview

We conducted a cohort study on datasets that contained times series data from electronic medical records of COVID-19 patients, whose overall workflow is illustrated in Fig. 1. Our goal was to establish a dynamic model for predicting the change in patients' conditions (mild, moderate, severe, critical, and death) using daily multidimensional data for COVID-19 patients. Two types of prediction models were constructed based on changes in patients' conditions: prediction of deterioration and prediction of recovery. After filling of missing data, dataset construction (including label of classification), variable engineering, feature selection, and comparison of different machine learning algorithms, the best algorithm was chosen to build the final model.

2.2. Study design and population

This was a single-centre retrospective cohort study conducted at Peking Union Medical College Hospital from November 2nd, 2022, to January 13th, 2023, and included hospitalized COVID-19 patients (Fig. 1a). Confirmed cases were determined by positive COVID-19 nucleic acid or antigen tests or clinical symptom onset. Pregnant patients were excluded.

The baseline was defined as the day of infection onset (Fig. 1b). For patients who visited the hospital after infection, the onset day was defined as the date when the symptoms first occurred. For patients who became infected during the hospital stay, the day of positive nucleic acid testing was used as the onset day. This study ended on January 13th, 2023. For patients who had already been discharged or died before this date, the observation end time was defined as the time of discharge or death. For patients who were still in the hospital on this date, the observation end time was defined as this day.

2.3. Outcome

This study used patient deterioration or recovery as the primary outcome (Fig. 1b). According to the "10th edition of the diagnosis and treatment protocol for COVID-19" in China (Diagnosis and Treatment Protocol for, 2023), patients' conditions were classified as mild, moderate, severe, or critical on every in-hospital day. Two dynamic prediction models were defined

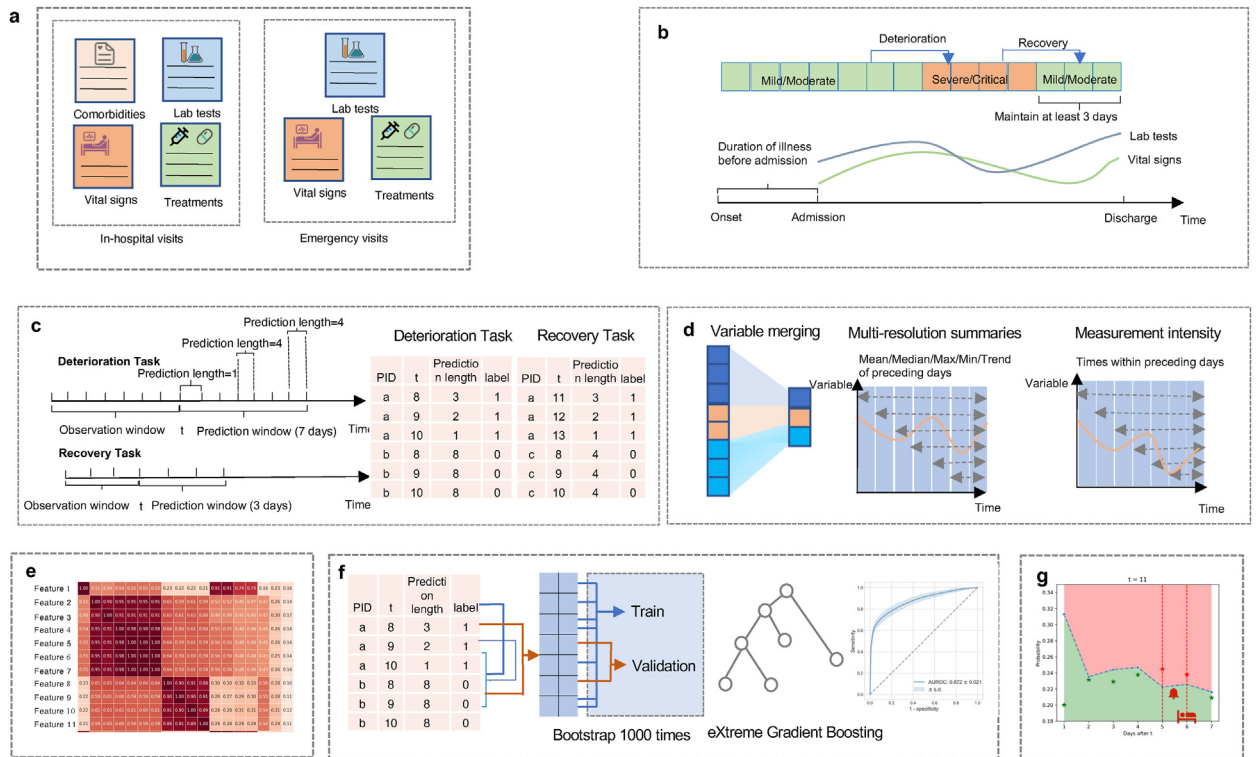


Fig. 1. Workflow of study.

a. Extraction of electronic health records. Electronic health records including comorbidities, laboratory test, vital sings, medications, and other treatments were extracted both for in-hospital visits and emergency visits. b. Outcome definition. c. Dataset construction. d. Feature engineering. e. Feature selection. f. Model construction and evaluation. g. Model application.

based on changes in patients' conditions: 1) prediction of deterioration: for patients categorized as having a mild or moderate condition at the observation time, whether the patient would deteriorate to a severe or critical condition or death in the following 7 days was predicted; and 2) prediction of recovery: for patients categorized as having a severe or critical condition at the observation time, whether the patient would recover to a mild or moderate condition in the following 3 days and maintain a mild or moderate condition for at least 3 days after recovery were predicted.

2.4. Variables

The study variables were obtained from the electronic medical record system (Fig. 1a) and included both baseline variables and time series of multidimensional variables. Baseline variables consisted of demographic information, personal history, history of COVID-19 vaccination, and comorbidities. Daily recorded longitudinal variables included laboratory test results, vital signs and treatments. The comprehensive variable list can be found in [Supplementary Table S1](#).

2.5. Filling of missing data

For missing data of laboratory tests and vital signs, for each valid measurement result, if there was no value after the time of this measurement, the valid measurement result would be filled for up to 2 days after the valid measurement. If there was a new valid measurement within 2 days, the filling would be terminated.

2.6. Dataset construction (including label of classification)

Since this study focused on dynamic changes occurring in patients, we generated datasets consisting of observations (Fig. 1c). One observation was generated for each patient at midnight every day during the course of COVID-19, consisting of all baseline and dynamic features within the previous seven/three (for deterioration and recovery prediction respectively) days.

For the deterioration prediction modelling procedure, only observations in which patients were in a mild or moderate state were included. An observation was marked as a positive label of classification, if the patient would deteriorate to a severe condition, critical condition or death in the following 7 days; otherwise, the label of observation was negative.

To predict not only whether an observation had a positive label but also on which day the positive label (deterioration) occurred, the full observation dataset was divided into seven sub-datasets based on the occurrence time of the positive label (referred as “prediction length”, in units of days). The negative observations in all seven sub-datasets were the same, i.e., those with negative labels (no deterioration in the next seven days).

Similar procedures applied to recovery prediction (refer to S1.2 of the Supplementary Materials for more details on recovery prediction modeling).

2.7. Variable engineering and feature selection

Medication variables were merged into antiviral, corticosteroid, and vasoactive drugs (variable merging in Fig. 1d, Supplementary Table S1). Multiresolution variables were generated from raw longitudinal variables (Fig. 1d), referring to S1.3 of the Supplementary Materials for details.

Spearman correlation analysis was used to analyze inter-feature dependencies (Supplementary Figs. S5–S10). During feature selection, a combined approach considering both correlation from data and the definition of each variable was adopted; only representative features were retained among strongly collinear variables (Fig. 1e for illustration, Supplementary Figs. S11–S12 for correlations of selected variables; refer to S1.4 of the Supplementary Materials for details).

2.8. Model development and evaluation

Six widely used algorithms, including extreme gradient boosting (XGBoost) (Chen & Guestrin, 2016), logistic regression (LR), support vector machines (SVM), decision tree (DT), random forest (RF), and neural network (NN), were used to develop the prediction model. Because the missing data could not be directly used by those algorithm implementations except XGBoost, multiple imputations were conducted according to the following steps. First, based on the original dataset, features with more than 30% missing values were removed from the analysis, to avoid unreliable imputation. Secondly, the remaining features with equal or less than 30% missing values were imputed by the multivariate imputation by the chained equation (MICE) method. We then selected the best-performing XGBoost algorithm to construct the final model (Fig. 1f).

To develop this model, on each sub-dataset (defined by prediction length), one separate prediction model was trained and evaluated using 1000 bootstrap iterations. The area under the receiver operating characteristic (ROC) curve (AUROC) was used as the performance evaluation metric. The AUROC was strictly evaluated on validation sets in the bootstrap method to avoid estimation caused by overfitting. In every bootstrap iteration, we randomly sampled with replacements to form a training set and used the remained unselected as validation set (Fig. 1f). The means and standard deviations of the AUROCs were calculated based on 1000 bootstrap iterations.

For case study and feature inspection, patients for each model were randomly divided into training and validation sets in a 7:3 ratio. The training set was used for variable inspection, while the validation set was used for a case study. In the case study, the optimal threshold was chosen by ensuring a sensitivity ≥ 0.6 for both the deterioration and recovery prediction models (Fig. 1g). Model-based predictive probabilities and actual changes in disease condition were drawn to visualize the individual-level application of the model. To inspect features, the Shapley additive explanations (SHAP) method and dependency plot were used to analyze the relationship between features and outcomes. A Venn plot and box plot of SHAP values were employed to illustrate the interaction effects between important comorbidities and the relationship between important comorbidities and the outcome.

2.9. Statistical analysis

Continuous variables are presented as medians and interquartile ranges (IQRs), which were compared using the Kruskal-Wallis test. Categorical variables are expressed as numbers and percentages (%). Pearson's χ^2 test or Fisher's exact test were used for categorical data, as appropriate. All p values were 2-tailed, and a p value < 0.05 was considered statistically significant. Statistical analyses were performed in Python 3.9 and R4.2.2.

3. Results

3.1. Study population

A total of 995 patients were eligible for inclusion in this study. The median age of the cohort was 67 years. According to the most severe condition during the disease course, 507 patients were mild or moderate, 308 patients were severe, 110 patients were critical, and 70 patients died. The baseline characteristics are shown in Table 1. A total of 604 patients were eligible for the deterioration prediction model, and 445 patients were eligible for the recovery prediction model.

3.2. Dataset construction and variable selection

A total of 7228 and 3170 observations were included for the deterioration and recovery prediction models, respectively. A total of 192 variables were selected for the deterioration model, and 88 variables were selected for the recovery model. The full list of selected variables can be found in [Supplementary Tables S2–S3](#). The correlation of the selected variables, which appears at least once in the top 10 important variables in different prediction lengths, are much lower than those before feature selection ([Supplementary Figs. S11–S12](#)).

3.3. Model evaluation

The results of different algorithms are shown in [Table 2](#). Of the considered machine learning algorithms, the XGBoost performed better than other algorithms in most prediction lengths in both deterioration and recovery prediction. To improve the usability of clinical application, as not all variables were available every day, we selected the algorithm XGBoost to build the final model on the dataset without multiple imputation.

For the deterioration prediction models, bootstrap validation showed that the AUROC of a prediction one day in advance was 0.872 (95% confidence interval (CI) 0.831–0.913), while that of a prediction seven days in advance was 0.786 (95% CI 0.721–0.851), with a daily AUROC exceeding 0.786 throughout the entire prediction window ([Fig. 2a](#), [Supplementary Fig. S13](#), [Table S4](#)). On the model developed by random splitting, the optimal thresholds were 0.298, 0.230, 0.231, 0.232, 0.212, 0.209, and 0.202 for predicting the next 7 days.

In case study of deterioration prediction task, patient b1 in the test set experienced a deterioration event at $t = 15$ ([Fig. 2 b1](#)). As the observation time approached the event time (from $t = 9$ to $t = 15$ in [Fig. 2 b1](#)), the model could predict the risk more accurately. For patient B2, the model correctly predicted low risk for the next 7 days, regardless of the observation time ([Fig. 2 b2](#)).

For the recovery prediction models, bootstrap validation showed that the AUROC of a prediction one day in advance was 0.823 (95% CI 0.770–0.876), while that of a prediction three days in advance was 0.675 (95% CI 0.583–0.767) ([Fig. 2c](#), [Supplementary Table S4](#)). On the model developed by random splitting, the optimal thresholds were 0.292, 0.235, and 0.201 for predicting the next 3 days.

In the case study of the recovery prediction task, patient d1 in the test set had a recovery event at $t = 8$, which lasted until $t = 10$ ([Fig. 2 d1](#)). As the observation time approached the event time, the model was able to predict the risk more accurately. For patient d2, the model correctly predicted low risk for the next three days, regardless of the observation time ([Fig. 2 d2](#)).

3.4. Feature inspection

The features with an important impact on predicting deterioration 1–7 days in advance were comorbidities, disease course, temperature, respiratory rate, and blood pressure ([Supplementary Figs. S14–S21](#)). Those that had an important impact on predicting recovery 1–3 days in advance were age, recent condition, disease course and observation time, treatments, and lymphocyte, D-dimer, and creatine levels ([Supplementary Figs. S22–S25](#)).

[Fig. 3a](#) illustrates the important features, taking the prediction of deterioration in the next 7 days as an example. In [Fig. 3b](#), dependency plots of the important continuous variables from [Fig. 3a](#) are presented. Similarly, [Fig. 3c](#) and [d](#) report important variables and dependency plots for predicting recovery in the next 3 days.

Regarding the deterioration prediction model, the population distribution between important comorbidities and box plots of their SHAP values can be seen in [Fig. 4](#).

4. Discussion

In this research, we retrospectively collected data on 995 hospitalized Omicron patients in China during the outbreak from Nov. 2022 to Jan. 2023. Based on the multidimensional longitudinal clinical data series of each patient, we established and internally validated prediction models for dynamically predicting the following at any observed time during the disease course: 1) the risk of deterioration from mild or medium to severe or critical in the next 7 days and 2) the possibility of recovery from severe or critical to mild or medium in the following 3 days. Additionally, within the explainable machine learning framework, some important features were identified, including both baseline comorbidities and dynamic clinical manifestations until the observation time. The models developed can be integrated as a tool system to assist clinicians in the ICU in dynamically evaluating the possibility of condition changes in the medium term (7 days or 3 days), thus potentially helping improve the prognosis of Omicron-infected hospitalized patients.

Although predicting the risks of COVID-19 patients by machine learning has been intensively studied since 2020, our work went beyond existing frontiers by introducing multidimensional daily clinical data series as predictors, establishing models using an ensemble machine learning approach to dynamically predict deterioration or recovery during the disease course, and validating the models to prove their effective discrimination capabilities.

Kogan et al. first developed a dynamic machine learning model for alerting of the imminent deterioration of hospitalized COVID-19 patients using longitudinal values of eight routinely collected laboratory test results ([Kogan et al., 2022](#)). However, the patient's clinical condition changes could not only be determined by daily laboratory test results but also need to consider

Table 1
Baseline characteristics of included Omicron patients.

Characteristics	Total	Mild/Moderate (n = 507)	Severe (n = 308)	Critical (n = 110)	Death (n = 70)	P value
Gender (Male)	568 (57.1)	269 (53.1)	176 (57.1)	81 (73.6)	42 (60)	<0.001
Age median (IQR)	67 (53,79)	64 (49,77)	68.5 (57,79)	66.5 (50.2,76)	79 (65.2,86)	<0.001
Hospitalization total duration median (IQR)	8 (4,15)	7 (3,15)	9 (6,15)	12 (5,23)	4 (2,9.8)	<0.001
Duration of infectivity median (IQR)	16 (5,24)	14 (3,24)	18 (8,23)	20 (7,28.8)	11 (4.2,19.2)	<0.001
Obesity	24 (2.4)	13 (2.6)	5 (1.6)	5 (4.5)	1 (1.4)	0.388
Smoker						<0.001
Missing	172 (17.3)	80 (15.8)	38 (12.3)	31 (28.2)	23 (32.9)	
Yes	233 (23.4)	113 (22.3)	72 (23.4)	31 (28.2)	17 (24.3)	
Vaccinated						<0.001
Missing	65 (6.5)	57 (11.2)	4 (1.3)	3 (2.7)	1 (1.4)	
Yes	106 (10.7)	50 (9.9)	43 (14)	10 (9.1)	3 (4.3)	
Hypertension	258 (25.9)	90 (17.8)	112 (36.4)	21 (19.1)	35 (50)	<0.001
Coronary heart disease	103 (10.4)	25 (4.9)	51 (16.6)	9 (8.2)	18 (25.7)	<0.001
Hyperlipidemia	115 (11.6)	48 (9.5)	52 (16.9)	7 (6.4)	8 (11.4)	0.003
Hypoalbuminemia	22 (2.2)	3 (0.6)	10 (3.2)	1 (0.9)	8 (11.4)	<0.001
Homeostatic imbalance	77 (7.7)	18 (3.6)	35 (11.4)	12 (10.9)	12 (17.1)	<0.001
Immune system disease	14 (1.4)	10 (2)	4 (1.3)	0 (0)	0 (0)	0.452
Respiratory system disease	479 (48.1)	168 (33.1)	180 (58.4)	72 (65.5)	59 (84.3)	<0.001
Neurological disease	89 (8.9)	34 (6.7)	36 (11.7)	7 (6.4)	12 (17.1)	0.005
Endocrine disease	296 (29.7)	122 (24.1)	113 (36.7)	29 (26.4)	32 (45.7)	<0.001
HIV	3 (0.3)	0 (0)	3 (1)	0 (0)	0 (0)	0.134
Digestive failure	260 (26.1)	115 (22.7)	98 (31.8)	26 (23.6)	21 (30)	0.027
Common Orthopedic disorder	140 (14.1)	65 (12.8)	49 (15.9)	12 (10.9)	14 (20)	0.216
Hematological disease	149 (15)	69 (13.6)	42 (13.6)	18 (16.4)	20 (28.6)	0.009
Urogenital disease	221 (22.2)	85 (16.8)	71 (23.1)	33 (30)	32 (45.7)	<0.001
Cancer	242 (24.3)	134 (26.4)	71 (23.1)	19 (17.3)	18 (25.7)	0.209
Lung cancer	50 (5)	23 (4.5)	17 (5.5)	6 (5.5)	4 (5.7)	0.914
Hematological malignancies	44 (4.4)	30 (5.9)	10 (3.2)	2 (1.8)	2 (2.9)	0.145
T_stage (Hematological malignancies = 0)						0.004
Missing	54 (27.3)	21 (20.2)	19 (31.1)	6 (35.3)	8 (50)	
Tis	2 (1)	0 (0)	1 (1.6)	0 (0)	1 (6.2)	
T1	44 (22.2)	20 (19.2)	21 (34.4)	3 (17.6)	0 (0)	
T2	32 (16.2)	18 (17.3)	9 (14.8)	2 (11.8)	3 (18.8)	
T3	30 (15.2)	21 (20.2)	6 (9.8)	1 (5.9)	2 (12.5)	
T4	36 (18.2)	24 (23.1)	5 (8.2)	5 (29.4)	2 (12.5)	
N_stage (Hematological malignancies = 0)						0.108
Missing	65 (32.8)	28 (26.9)	22 (36.1)	6 (35.3)	9 (56.2)	
N0	61 (30.8)	29 (27.9)	25 (41)	3 (17.6)	4 (25)	
N1	29 (14.6)	19 (18.3)	6 (9.8)	3 (17.6)	1 (6.2)	
N2	25 (12.6)	19 (18.3)	3 (4.9)	2 (11.8)	1 (6.2)	
N3	18 (9.1)	9 (8.7)	5 (8.2)	3 (17.6)	1 (6.2)	
M_stage (Hematological malignancies = 0)						0.439
Missing	37 (18.7)	16 (15.4)	14 (23)	3 (17.6)	4 (25)	
M0	105 (53)	56 (53.8)	35 (57.4)	8 (47.1)	6 (37.5)	
M1	56 (28.3)	32 (30.8)	12 (19.7)	6 (35.3)	6 (37.5)	
Clinical_stage (Hematological malignancies = 0)						<0.001
Missing	54 (27.3)	20 (19.2)	24 (39.3)	4 (23.5)	6 (37.5)	
0	2 (1)	0 (0)	1 (1.6)	0 (0)	1 (6.2)	
I	31 (15.7)	16 (15.4)	14 (23)	1 (5.9)	0 (0)	
II	21 (10.6)	7 (6.7)	9 (14.8)	2 (11.8)	3 (18.8)	
III	37 (18.7)	28 (26.9)	5 (8.2)	3 (17.6)	1 (6.2)	
IV	53 (26.8)	33 (31.7)	8 (13.1)	7 (41.2)	5 (31.2)	

multidimensional variables on each day, including viral infection reflected by the disease course, the patient's underlying condition and organ dysfunction reflected by vital signs and laboratory tests, and the timing, manner, and intensity of clinical treatments. Predictive models can only produce scientific, accurate and up-to-date results if risk forecasts are updated daily with the full set of factors.

Therefore, thanks to the complete range of variables, we were able to extend the deterioration prediction range from two to four days to seven days, compared with the study by Kogan et al. Using higher dimension parameters, our models' AUROCs (0.872, 0.801, 0.807 and 0.819 from the following 1–4 days, respectively) exceeded their internal validated result (0.80 in 2 days/0.79 in 4 days).

In addition, forecasting whether the patient's condition could be improved in the next few days is useful for those who already have a severe condition. However, to our knowledge, this has not yet been reported. Although the AUROC of recovery in the next 3 days was limited (0.675) in this study, the AUROC of recovery on the next day was satisfactory (0.823), paving the way for refined recovery assessment research in the future.

Table 2
Six algorithms' AUROC (95% Confidence Interval) of deterioration and recovery prediction.

Prediction Model	prediction length (days)	XGBoost	Logistic Regression	Support Vector Machines	Decision Tree	Random Forest	Neutral Network
Deterioration Prediction Model	1	0.899 (0.867, 0.930)	0.839 (0.809, 0.870)	0.840 (0.809, 0.878)	0.855 (0.820, 0.878)	0.828 (0.793, 0.869)	0.833 (0.797, 0.876)
	2	0.823 (0.783, 0.855)	0.835 (0.788, 0.871)	0.836 (0.788, 0.874)	0.787 (0.741, 0.826)	0.800 (0.748, 0.838)	0.808 (0.755, 0.846)
	3	0.819 (0.764, 0.857)	0.793 (0.731, 0.829)	0.801 (0.741, 0.837)	0.789 (0.737, 0.843)	0.800 (0.744, 0.841)	0.799 (0.723, 0.855)
	4	0.832 (0.784, 0.878)	0.794 (0.759, 0.831)	0.805 (0.762, 0.842)	0.795 (0.725, 0.850)	0.818 (0.782, 0.850)	0.806 (0.758, 0.847)
	5	0.799 (0.743, 0.850)	0.753 (0.697, 0.801)	0.759 (0.719, 0.817)	0.765 (0.715, 0.843)	0.794 (0.749, 0.836)	0.764 (0.696, 0.825)
	6	0.799 (0.735, 0.845)	0.754 (0.673, 0.814)	0.756 (0.690, 0.801)	0.765 (0.690, 0.821)	0.799 (0.737, 0.858)	0.764 (0.689, 0.837)
	7	0.800 (0.739, 0.866)	0.764 (0.681, 0.827)	0.763 (0.690, 0.818)	0.741 (0.637, 0.802)	0.804 (0.738, 0.870)	0.768 (0.671, 0.853)
Recovery Prediction Model	1	0.811 (0.766, 0.850)	0.793 (0.750, 0.837)	0.806 (0.763, 0.849)	0.725 (0.671, 0.815)	0.792 (0.736, 0.835)	0.794 (0.730, 0.848)
	2	0.751 (0.690, 0.814)	0.727 (0.652, 0.792)	0.738 (0.672, 0.814)	0.660 (0.568, 0.745)	0.740 (0.668, 0.825)	0.728 (0.674, 0.802)
	3	0.649 (0.580, 0.717)	0.621 (0.529, 0.728)	0.643 (0.567, 0.732)	0.558 (0.412, 0.665)	0.650 (0.568, 0.724)	0.625 (0.504, 0.737)

Prediction length (days): duration between observation and positive outcome within prediction window.
The **italic bold number** means the best mean AUROC at the prediction length of prediction model.

Within the explainable machine learning framework, we identified important factors associated with deterioration or recovery of patients' conditions in the next few days.

Age and disease course were important predictors for both models. There is a consensus that younger people are more likely to recover, so no further elaboration is needed. In particular, we found that the first 10 days of the disease course should be of great concern, given that patients had a higher risk of deterioration or were more likely to recover during this period. The early stage of the disease is essential for the body's immune response, and Lucas et al. Indicated that major differences in immune phenotypes between moderate and severe disease become apparent after day 10 of infection (Lucas et al., 2020). In addition, a long disease course usually indicates delayed viral clearance, leading to vascular damage and impaired tissue repair (Merad et al., 2022); therefore, the first 10 days of the disease course are noteworthy for physicians, and timely interventions are crucial to the patient's prognosis.

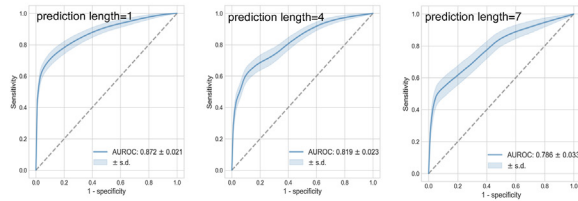
In the deterioration prediction model, the most important predictive features were vital signs, including body temperature, respiratory rate, and blood pressure, which could reflect the patient's disease condition in real time and were more sensitive than the lagging laboratory results.

In terms of comorbidities, this study confirmed the well-known findings that hypertension, coronary heart disease and diabetes are essential to the severity of COVID-19. More interestingly, hyperlipidemia was found to be a risk factor for worsening in the next 1–7 days. Additionally, the importance of hyperlipidemia was independent of some potential known confounders (Fig. 4). A previous cross-sectional study found that the presence of atherosclerotic dyslipidemia (low high-density lipoprotein and high triglyceride levels) during infection was independently associated with a worse prognosis in COVID-19 infection (Masana et al., 2021), and we also found that hyperlipidemia strongly impacted the deterioration of COVID-19 patients. High cholesterol can facilitate the SARS-CoV-2 host cell infection process mediated by viral spike protein (SARS-2-S) and angiotensin-converting enzyme 2 (ACE2) receptor attachment by increasing plasma membrane lipid raft density and directly binding viral proteins (Radenkovic et al., 2020; Wei et al., 2020). Dias et al. found that the use of a DGAT-1 (a key enzyme in triacylglycerol synthesis) inhibitor during SARS-CoV-2 infection decreased the viral load in monocytes by reducing lipid droplet biogenesis (Dias et al., 2020). Therefore, hyperlipidemia deserves as much attention as other comorbidities.

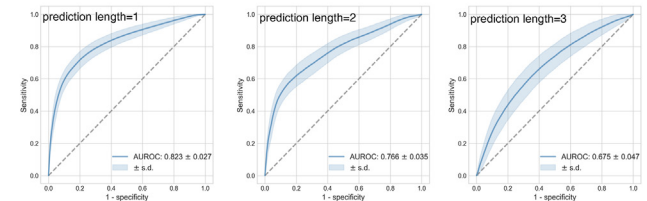
In the recovery prediction model, the important predictive features also included D-dimer levels, oxygen inhalation, extracorporeal membrane oxygenation (ECMO), and corticosteroid therapy.

Patients with normal D-dimer levels were more likely to improve. Our team identified coagulopathy in patients with COVID-19 in early 2020 (Zhang, Xiao, et al., 2020), and abnormal D-dimer values were found to be independently associated with critical illness, thrombotic events, acute kidney injury, and all-cause mortality (Berger et al., 2020). With normal fibrinogen and platelet levels, elevated circulating D-dimer (reflecting pulmonary vascular bed thrombosis with fibrinolysis) was an important early feature of severe pulmonary intravascular coagulopathy in COVID-19 (McGonagle et al., 2020). Therefore, monitoring of patients' D-dimer levels is important in clinical practice, and the conditional use of prophylactic anticoagulation for critically ill patients has been recommended by guidelines (Cuker et al., 2022; Therapeutics and COVID, 2023).

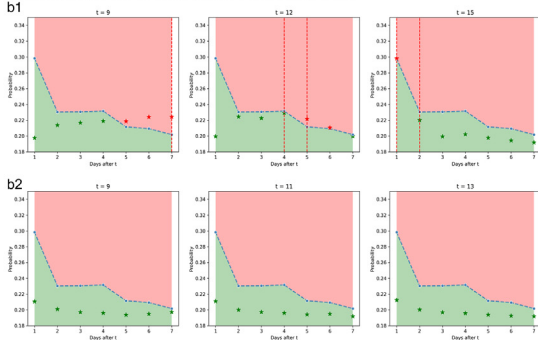
a ROC of Deterioration Prediction Model at different prediction lengths



c ROC of Recovery Prediction Model at different prediction lengths



b Case study on Deterioration Prediction Task



d Case study on Recovery Prediction Task

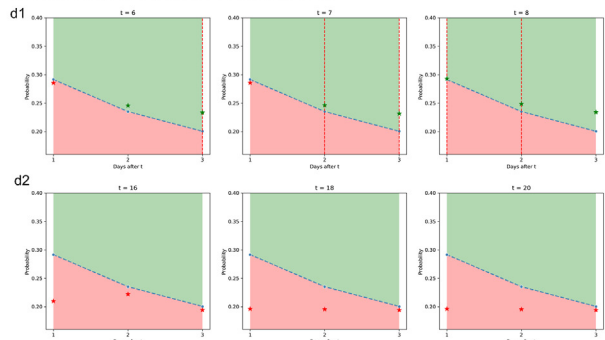
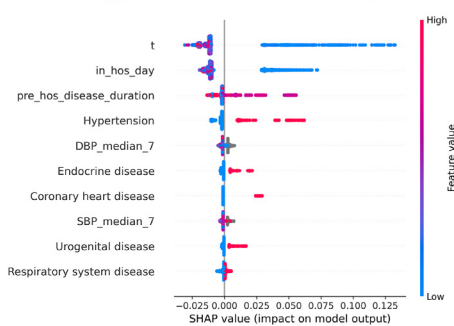


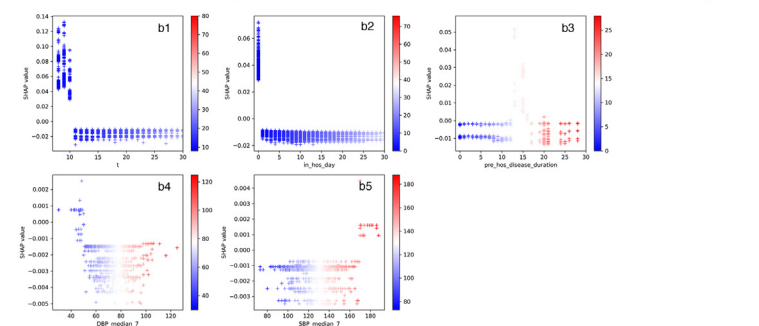
Fig. 2. Model performance at population and individual level.

a/c. prediction length: duration between observation and positive outcome within prediction window. ROC: Receiver-operating characteristic curve. ROCs of other prediction lengths were shown in supplementary material. **b.** The blue dotted line represents the risk threshold, dividing the graph into two regions. Red represents high risk, and green represents low risk. The star points represent predicted values. The red dotted line perpendicular to the x-axis represents occurrence of target outcome at that day. **b1** and **b2** represent different individual, respectively. **d.** The blue dotted line represents the risk threshold, dividing the graph into two regions. Green represents high risk, and red represents low risk. The star points represent predicted values. The red dotted line perpendicular to the x-axis represents occurrence of target outcome at that day. **d1** and **d2** represent different individual, respectively.

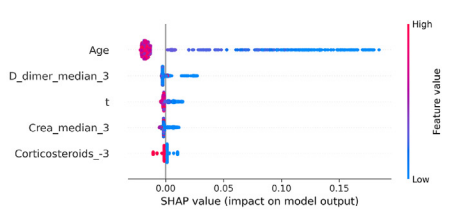
a SHAP summary plot of Deterioration Prediction Model at prediction length=7



b SHAP Dependence plot for the top 10 continuous features of Deterioration Prediction Model at prediction length=7



c SHAP summary plot of Recovery Prediction Model at prediction length=3



d SHAP Dependence plot of Recovery Prediction Model at prediction length=3

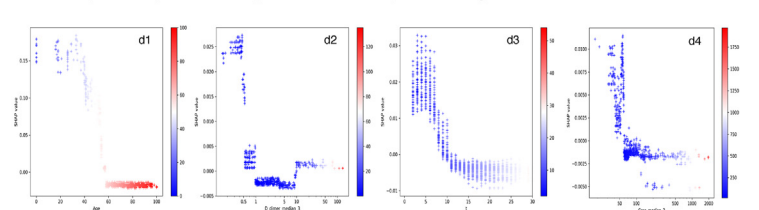


Fig. 3. Feature inspection.

b. the x-axis represents the actual values and the y-axis represents the SHAP values. Colorbar scale represents the actual values of feature, the greater the value, the redder the color. *Interpretation: in_hos_day: Time t is days after admission; t: observation time measured by length of disease duration; pre_hos_disease_duration: duration of disease before admission; SBP: systolic blood pressure for the preceding 7 days; DBP_median_7: diastolic blood pressure for the preceding 7 days; D_dimer_median_3: median D_dimer for the preceding 3 days; Crea_median_3: median creatinine for the preceding 3 days; Corticosteroids_3: whether corticosteroids were used 3 days before time t.

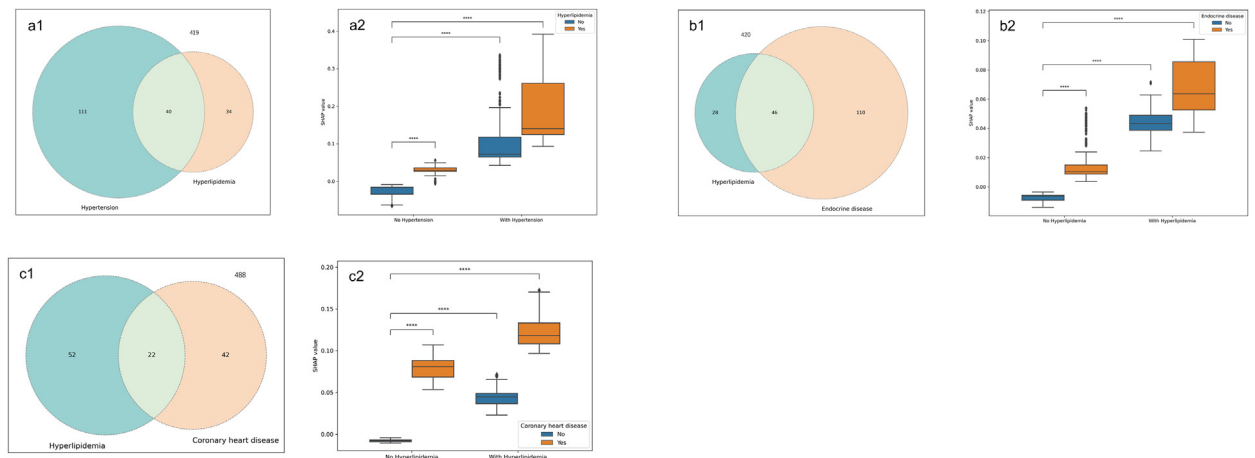


Fig. 4. Comorbidities inspection.

a1. Venn plot of hypertension and hyperlipidemia in Deterioration Task population. a2. Boxplot of SHAP values by hypertension and hyperlipidemia in Deterioration Task population. b1. Venn plot of hyperlipidemia and endocrine disease in Deterioration Task population. b2. Boxplot of SHAP values by hyperlipidemia and endocrine disease in Deterioration Task population. c1. Venn plot of hyperlipidemia and coronary heart disease in Deterioration Task population. c2. Boxplot of SHAP values by hyperlipidemia and coronary heart disease in Deterioration Task population. (a1). Combined with hypertension: 151; combined with hyperlipidemia: 74; combined with hypertension and hyperlipidemia: 40; combined with neither hypertension nor hyperlipidemia: 419. (b1). Combined with hyperlipidemia: 74; combined with endocrine disease: 156; combined with hyperlipidemia and endocrine disease: 46; combined with neither hyperlipidemia nor endocrine disease: 420. (c1). Combined with hyperlipidemia: 74; combined with coronary heart disease: 64; combined with hyperlipidemia and coronary heart disease: 22; combined with neither hyperlipidemia nor coronary heart disease: 488. (a2/b2/c2). ****: $p \leq 1.00 \text{ E-}04$.

In this cohort, 41.2% of the patients received corticosteroid therapy, and 43.9% of the patients received oxygen therapy. Corticosteroids, although RECOVERY trials proved their clinical benefits for severe COVID-19 patients (Group et al., 2021; Group WHOReAfc-TW et al., 2020) and are recommended by guidelines (Li et al., 2023), are still under debate regarding their therapeutic effects. Compared to monoclonal antibodies, whose administration for specific groups only should be closely monitored based on serum-targeting ligand levels (Bhimraj et al., 2022) and to date do not cover Omicron variants (Cao et al., 2022), corticosteroids are highlighted for their systemic effects in the body, downregulating interferon-stimulated genes and altering cellular interactions by acting on neutrophil maturation (Sinha et al., 2022), as delayed interferon responses and the formation of neutrophil extracellular traps (NETs) might contribute to organ damage and mortality in COVID-19 (Barnes et al., 2020; Zhang, Bastard, et al., 2020). However, the anti-inflammatory and immunomodulatory effects (Sinha et al., 2022) of corticosteroids suppress immune responses and have been shown to lead to prolonged clearance of viral RNA from patients' airways (Arabi et al., 2018), blood (Lee et al., 2004), and faeces (Ling et al., 2020) in previous studies that focused on other viruses. This is why the CIBERESUCICOVID study found that corticosteroids might prove harmful for COVID-19 patients (Torres et al., 2022). Thus, the use of corticosteroids is controversial, and more plausible trials are needed in this field. Our study, as a large observational study at a national medical centre where a substantial portion of patients were given corticosteroids during their illness, demonstrated the benefit of corticosteroids in the improvement of severely ill patients, informing the usage of corticosteroids for Omicron patients.

COVID-19 patients often have remarkably low oxygen saturation levels but no dyspnoea, as did patients in our cohort, which is called "silent hypoxemia" (Tobin et al., 2020) and poses a challenge to clinicians. Hypoxemia causes damage to cells, leading to lysis and necrosis of cells and surrounding tissues, resulting in organ dysfunction and even failure. Multiple patients in our trial received oxygen therapy after admission, confirming its efficacy in rescuing them from critical illness. Hence, early diagnosis and timely administration of oxygen therapy is a wise strategy.

The proposed models are practical in clinical practice. In Fig. 2b and d, the simulated application results of selected patients demonstrated that the models could aid clinical decision-making by forecasting deterioration or recovery events proactively and reliably. At the practice level, although the requirements for longitudinal multidimensional predictors seem complex, by integrating the proposed models into the hospital information system, clinicians could obtain prediction results automatically. Finally, all predictors in the proposed models are easily accessible during routine clinical processes, which ensures that the models are applicable across medical centres of different levels.

This study had several limitations. First, it was a single-centre retrospective study. Validation in external centres is being planned. Additionally, to evaluate the extent to which patients actually benefit from model-assisted decision-making, prospective studies in our and external centres will be our next step. Second, limited by the granularity of clinical conditions in the guidelines (mild, moderate, severe, and critical), this study only predicted the progression of patients' conditions from mild/moderate to severe/critical (and vice versa) but did not predict the possibility of patients' improvement or deterioration for any condition. As the most important goal of COVID-19 clinical care is the prevention and management of severe or critical conditions, such limitations do not impair the applicability of the models for clinical use. Third, the algorithmic bias is

consequential and common when machine learning is used to develop a medical tool (Ferryman et al., 2023), as in our study. We will try to supplement the data from other medical centres in subsequent clinical practice, and keep revising the model to fix the bias.

Statements and declarations

No conflict of interest exists in the submission of this manuscript, and manuscript is approved by all authors for publication. I would like to declare on behalf of my co-authors that the work described was original research that has not been published previously, and not under consideration for publication elsewhere, in whole or in part. All the authors listed have approved the manuscript that is enclosed.

Ethics approval

This study was approved by the Ethics Committee of Peking Union Medical College Hospital (No. I-23PJ441).

Funding sources

National High Level Hospital Clinical Research Funding (2023-PUMCH-G-001), Chinese Academy of Medical Sciences and Peking Union Medical Hospital (K3872), Beijing Municipal Natural Science Foundation General Program (M21019) and Beijing Municipal Natural Science Foundation-Haidian Original Innovation Unite Foundation Key Program (L222019).

Declaration of competing interest

The authors declare that they have no known competing financial interests or personal relationships that could have appeared to influence the work reported in this paper.

Appendix A. Supplementary data

Supplementary data to this article can be found online at <https://doi.org/10.1016/j.idm.2023.09.003>.

References

- Arabi, Y. M., Mandourah, Y., Al-Hameed, F., Sindi, A. A., Almekhlafi, G. A., Hussein, M. A., Jose, J., Pinto, R., Al-Omari, A., Kharaba, A., Almotairi, A., Al Khatib, K., Alraddadi, B., Shalhoub, S., Abdulmomen, A., Qushmaq, I., Mady, A., Solaiman, O., Al-Aithan, A. M., ... Fowler, R. A., & Saudi Critical Care Trial G. (2018). Corticosteroid therapy for critically ill patients with Middle East respiratory syndrome. *American Journal of Respiratory and Critical Care Medicine*, 197, 757–767. <https://doi.org/10.1164/rccm.201706-1172OC>
- Assaf, D., Gutman, Y., Neuman, Y., Segal, G., Amit, S., Gefen-Halevi, S., Shilo, N., Epstein, A., Mor-Cohen, R., Biber, A., Rahav, G., Levy, I., & Tirosh, A. (2020). Utilization of machine-learning models to accurately predict the risk for critical COVID-19. *Intern Emerg Med*, 15, 1435–1443. <https://doi.org/10.1007/s11739-020-02475-0>
- Barnes, B. J., Adrover, J. M., Baxter-Stoltzfus, A., Borczuk, A., Cools-Lartigue, J., Crawford, J. M., Dassler-Plenker, J., Guerci, P., Huynh, C., Knight, J. S., Loda, M., Looney, M. R., McAllister, F., Rayes, R., Renaud, S., Rousseau, S., Salvatore, S., Schwartz, R. E., Spicer, J. D., ... Egeblad, M. (2020). Targeting potential drivers of COVID-19: Neutrophil extracellular traps. *Journal of Experimental Medicine*, 217. <https://doi.org/10.1084/jem.20200652>
- Berger, J. S., Kunichoff, D., Adhikari, S., Ahuja, T., Amoroso, N., Aphinyanaphongs, Y., Cao, M., Goldenberg, R., Hindenburg, A., Horowitz, J., Parnia, S., Petrilli, C., Reynolds, H., Simon, E., Slater, J., Yaghi, S., Yuriditsky, E., Hochman, J., & Horwitz, L. I. (2020). Prevalence and outcomes of D-dimer elevation in hospitalized patients with COVID-19. *Arteriosclerosis, Thrombosis, and Vascular Biology*, 40, 2539–2547. <https://doi.org/10.1161/ATVBAHA.120.314872>
- Bhimraj, A., Morgan, R. L., Shumaker, A. H., Baden, L., Cheng, V. C. C., Edwards, K. M., Gallagher, J. C., Gandhi, R. T., Muller, W. J., Nakamura, M. M., O'Horo, J. C., Shafer, R. W., Shoham, S., Murad, M. H., Mustafa, R. A., Sultan, S., & Falck-Ytter, Y. (2022). Infectious diseases society of America guidelines on the treatment and management of patients with COVID-19. *Clinical Infectious Diseases*. <https://doi.org/10.1093/cid/ciac724>
- Cao, Y., Wang, J., Jian, F., Xiao, T., Song, W., Yisimayi, A., Huang, W., Li, Q., Wang, P., An, R., Wang, J., Wang, Y., Niu, X., Yang, S., Liang, H., Sun, H., Li, T., Yu, Y., Cui, Q., ... Xie, X. S. (2022). Omicron escapes the majority of existing SARS-CoV-2 neutralizing antibodies. *Nature*, 602, 657–663. <https://doi.org/10.1038/s41586-021-04385-3>
- Chen, T., & Guestrin, C. (2016). XGBoost: A scalable tree boosting system. *ACM*, 785–794. <https://doi.org/10.1145/2939672.2939785>
- Cuker, A., Tseng, E. K., Schunemann, H. J., Angchaisuksiri, P., Blair, C., Dane, K., DeSancho, M. T., Diuguid, D., Griffin, D. O., Kahn, S. R., Klok, F. A., Lee, A. I., Neumann, I., Pai, A., Righini, M., Sanfilippo, K. M., Siegal, D. M., Skara, M., Terrell, D. R., ... Nieuwlaat, R. (2022). American Society of Hematology living guidelines on the use of anticoagulation for thromboprophylaxis for patients with COVID-19: March 2022 update on the use of anticoagulation in critically ill patients. *Blood Adv*, 6, 4975–4982. <https://doi.org/10.1182/bloodadvances.2022007940>
- Diagnosis and treatment protocol for novel coronavirus pneumonia (trial version 10). <http://www.gov.cn/zhengce/zhengceku/2023-01/06/5735343/files/5844ce04246b431dbd322d8ba10afb48.pdf>, (2023).
- Dias, S. G., Soares, V. C., Ferreira, A. C., Sacramento, C. Q., Fintelman-Rodrigues, N., Temerozo, J. R., Teixeira, L., Nunes da Silva, M. A., Barreto, E., Mattos, M., de Freitas, C. S., Azevedo-Quintanilha, I. G., Manso, P. P. A., Miranda, M. D., Siqueira, M. M., Hottz, E. D., Pao, C. R. R., Bou-Habib, D. C., Barreto-Vieira, D. F., ... Bozza, P. T. (2020). Lipid droplets fuel SARS-CoV-2 replication and production of inflammatory mediators. *PLoS Pathogens*, 16, Article e1009127. <https://doi.org/10.1371/journal.ppat.1009127>
- Ferryman, K., Drazen, J. M., Mackintosh, M., & Ghassemi, M. (2023). Considering biased data as informative artifacts in AI-assisted health care. *New England Journal of Medicine*, 389, 833–838. <https://doi.org/10.1056/NEJMra2214964>
- Gao, Y., Cai, G. Y., Fang, W., Li, H. Y., Wang, S. Y., Chen, L., Yu, Y., Liu, D., Xu, S., Cui, P. F., Zeng, S. Q., Feng, X. X., Yu, R. D., Wang, Y., Yuan, Y., Jiao, X. F., Chi, J. H., Liu, J. H., Li, R. Y., ... Gao, Q. L. (2020). Machine learning based early warning system enables accurate mortality risk prediction for COVID-19. *Nature Communications*, 11, 5033. <https://doi.org/10.1038/s41467-020-18684-2>
- Group, R. C., Horby, P., Lim, W. S., Emberson, J. R., Mafham, M., Bell, J. L., Linsell, L., Staplin, N., Brightling, C., Ustianowski, A., Elmahi, E., Prudon, B., Green, C., Felton, T., Chadwick, D., Rege, K., Fegan, C., Chappell, L. C., Faust, S. N., ... Landray, M. J. (2021). Dexamethasone in hospitalized patients with covid-19. *New England Journal of Medicine*, 384, 693–704. <https://doi.org/10.1056/NEJMoa2021436>

- Kogan, Y., Robinson, A., Itelman, E., Bar-Nur, Y., Jakobson, D. J., Segal, G., & Agur, Z. (2022). Developing and validating a machine learning prognostic model for alerting to imminent deterioration of hospitalized patients with COVID-19. *Scientific Reports*, 12, Article 19220. <https://doi.org/10.1038/s41598-022-23553-7>
- Lee, N., Allen Chan, K. C., Hui, D. S., Ng, E. K., Wu, A., Chiu, R. W., Wong, V. W., Chan, P. K., Wong, K. T., Wong, E., Cockram, C. S., Tam, J. S., Sung, J. J., & Lo, Y. M. (2004). Effects of early corticosteroid treatment on plasma SARS-associated Coronavirus RNA concentrations in adult patients. *Journal of Clinical Virology*, 31, 304–309. <https://doi.org/10.1016/j.jcv.2004.07.006>
- Li, G., Hilgenfeld, R., Whitley, R., & De Clercq, E. (2023). Therapeutic strategies for COVID-19: Progress and lessons learned. *Nature Reviews Drug Discovery*, 1–27. <https://doi.org/10.1038/s41573-023-00672-y>
- Ling, Y., Xu, S. B., Lin, Y. X., Tian, D., Zhu, Z. Q., Dai, F. H., Wu, F., Song, Z. G., Huang, W., Chen, J., Hu, B. J., Wang, S., Mao, E. Q., Zhu, L., Zhang, W. H., & Lu, H. Z. (2020). Persistence and clearance of viral RNA in 2019 novel coronavirus disease rehabilitation patients. *Chinese Medical Journal*, 133, 1039–1043. <https://doi.org/10.1097/CM9.0000000000000774>
- Lucas, C., Wong, P., Klein, J., Castro, T. B. R., Silva, J., Sundaram, M., Ellingson, M. K., Mao, T., Oh, J. E., Israelow, B., Takahashi, T., Tokuyama, M., Lu, P., Venkataraman, A., Park, A., Mohanty, S., Wang, H., Wyllie, A. L., Vogels, C. B. F., ... Iwasaki, A. (2020). Longitudinal analyses reveal immunological misfiring in severe COVID-19. *Nature*, 584, 463–469. <https://doi.org/10.1038/s41586-020-2588-y>
- Masana, L., Correig, E., Ibarretxe, D., Anoro, E., Arroyo, J. A., Jerico, C., Guerrero, C., Miret, M., Naf, S., Pardo, A., Perea, V., Perez-Bernalte, R., Plana, N., Ramirez-Montesinos, R., Royuela, M., Soler, C., Urquizu-Padilla, M., Zamora, A., Pedro-Botet, J., & S-Xr, group (2021). Low HDL and high triglycerides predict COVID-19 severity. *Scientific Reports*, 11, 7217. <https://doi.org/10.1038/s41598-021-86747-5>
- McGonagle, D., O'Donnell, J. S., Sharif, K., Emery, P., & Bridgewood, C. (2020). Immune mechanisms of pulmonary intravascular coagulopathy in COVID-19 pneumonia. *Lancet Rheumatol*, 2, e437–e445. [https://doi.org/10.1016/S2665-9913\(20\)30121-1](https://doi.org/10.1016/S2665-9913(20)30121-1)
- Merad, M., Blish, C. A., Sallusto, F., & Iwasaki, A. (2022). The immunology and immunopathology of COVID-19. *Science*, 375, 1122–1127. <https://doi.org/10.1126/science.abm8108>
- Radenkovic, D., Chawla, S., Pirro, M., Sahebkar, A., & Banach, M. (2020). Cholesterol in relation to COVID-19: Should we care about it? *Journal of Clinical Medicine*, 9. <https://doi.org/10.3390/jcm9061909>
- Sinha, S., Rosin, N. L., Arora, R., Labit, E., Jaffer, A., Cao, L., Farias, R., Nguyen, A. P., de Almeida, L. G. N., Dufour, A., Bromley, A., McDonald, B., Gillrie, M. R., Fritzier, M. J., Yipp, B. G., & Biernaskie, J. (2022). Dexamethasone modulates immature neutrophils and interferon programming in severe COVID-19. *Nat Med*, 28, 201–211. <https://doi.org/10.1038/s41591-021-01576-3>
- Group WHOAREfC-TW, Sterne, J. A. C., Murthy, S., Diaz, J. V., Slutsky, A. S., Villar, J., Angus, D. C., Annane, D., Azevedo, L. C. P., Berwanger, O., Cavalcanti, A. B., Dequin, P. F., Du, B., Emberson, J., Fisher, D., Giraudeau, B., Gordon, A. C., Granholm, A., Green, C., Haynes, R., ... Marshall, J. C. (2020). Association between administration of systemic corticosteroids and mortality among critically ill patients with COVID-19: A meta-analysis. *JAMA*, 324, 1330–1341. <https://doi.org/10.1001/jama.2020.17023>
- Therapeutics and COVID-19: Living guideline. <https://www.who.int/publications/i/item/WHO-2019-nCoV-therapeutics-2023.1>, (2023).
- Tobin, M. J., Laghi, F., & Jubran, A. (2020). Why COVID-19 silent hypoxemia is baffling to physicians. *American Journal of Respiratory and Critical Care Medicine*, 202, 356–360. <https://doi.org/10.1164/rccm.202006-2157CP>
- Torres, A., Motos, A., Cilloniz, C., Ceccato, A., Fernandez-Barat, L., Gabarrus, A., Bermejo-Martin, J., Ferrer, R., Riera, J., Perez-Arnal, R., Garcia-Gasulla, D., Penuelas, O., Lorente, J. A., de Gonzalo-Calvo, D., Almansa, R., Menendez, R., Palomeque, A., Villar, R. A., Anon, J. M., ... Investigators, C. P. (2022). Major candidate variables to guide personalised treatment with steroids in critically ill patients with COVID-19: CIBERESUCICOVID study. *Intensive Care Medicine*, 48, 850–864. <https://doi.org/10.1007/s00134-022-06726-w>
- Wei, C., Wan, L., Yan, Q., Wang, X., Zhang, J., Yang, X., Zhang, Y., Fan, C., Li, D., Deng, Y., Sun, J., Gong, J., Yang, X., Wang, Y., Wang, X., Li, J., Yang, H., Li, H., Zhang, Z., ... Zhong, H. (2020). HDL-scavenger receptor B type 1 facilitates SARS-CoV-2 entry. *Nature Metabolism*, 2, 1391–1400. <https://doi.org/10.1038/s42255-020-00324-0>
- Zhang, Q., Bastard, P., Liu, Z., Le Pen, J., Moncada-Velez, M., Chen, J., Ogishi, M., Sabli, I. K. D., Hodeib, S., Korol, C., Rosain, J., Bilguvar, K., Ye, J., Bolze, A., Bigio, B., Yang, R., Arias, A. A., Zhou, Q., Zhang, Y., Onodi, F., Korniotis, S., Karpf, L., Philippot, Q., Chbihi, M., Bonnet-Madin, L., Dorgham, K., Smith, N., Schneider, W. M., Razoooky, B. S., Hoffmann, H. H., Michailidis, E., Moens, L., Han, J. E., Lorenzo, L., Bizien, L., Meade, P., Neehus, A. L., Ugurbil, A. C., Corneau, A., Kerner, G., Zhang, P., Rapaport, F., Seeleuthner, Y., Manry, J., Masson, C., Schmitt, Y., Schluter, A., Le Voyer, T., Khan, T., Li, J., Fellay, J., Roussel, L., Shahrooei, M., Alosaimi, M. F., Mansouri, D., Al-Saud, H., Al-Mulla, F., Almourfi, F., Al-Muhsen, S. Z., Alosaime, F., Al Turki, S., Hasanato, R., van de Beek, D., Biondi, A., Bettini, L. R., D'Angio, M., Bonfanti, P., Imberti, L., Sottini, A., Paghera, S., Quiros-Roldan, E., Rossi, C., Oler, A. J., Tompkins, M. F., Alba, C., Vandernoot, I., Goffard, J. C., Smits, G., Migeotte, I., Haerynck, F., Soler-Palacin, P., Martin-Nalda, A., Colobran, R., Morange, P. E., Keles, S., Colkesen, F., Ozelik, T., Yasar, K. K., Senoglu, S., Karabela, S. N., Rodriguez-Gallego, C., Novelli, G., Hraiech, S., Tandjaoui-Lambiotte, Y., Duval, X., Laouenan, C., Clinicians C-S, Clinicians C, Imagine CG, French CCSG, Co VCC, Amsterdam UMCC-B, Effort CHG, Group N-UTCI, Snow, A. L., Dalgard, C. L., Milner, J. D., Vinh, D. C., Mogensen, T. H., Marr, N., Spaan, A. N., Boisson, B., Boisson-Dupuis, S., Bustamante, J., Puel, A., Ciancanelli, M. J., Meyts, I., Maniatis, T., Soumelis, V., Amara, A., Nussenzweig, M., Garcia-Sastre, A., Krammer, F., Pujol, A., Duffy, D., Lifton, R. P., Zhang, S. Y., Gorochov, G., Beziat, V., Jouanguy, E., Sancho-Shimizu, V., Rice, C. M., Abel, L., Notarangelo, L. D., Cobat, A., Su, H. C., & Casanova, J. L. (2020). Inborn errors of type 1 IFN immunity in patients with life-threatening COVID-19. *Science*, 370. <https://doi.org/10.1126/science.abd4570>
- Zhang, Y., Xiao, M., Zhang, S., Xia, P., Cao, W., Jiang, W., Chen, H., Ding, X., Zhao, H., Zhang, H., Wang, C., Zhao, J., Sun, X., Tian, R., Wu, W., Wu, D., Ma, J., Chen, Y., Zhang, D., ... Zhang, S. (2020). Coagulopathy and antiphospholipid antibodies in patients with covid-19. *New England Journal of Medicine*, 382, e38. <https://doi.org/10.1056/NEJMc2007575>